Photon Condensation and Enhanced Magnetism in Cavity QED

Juan Román-Roche, Fernando Luis, and David Zueco
Instituto de Nanociencia y Materiales de Aragón (INMA) and Departamento de Física de la Materia Condensada, CSIC-Universidad de Zaragoza, Zaragoza 50009, Spain

(Received 1 December 2020; revised 25 August 2021; accepted 25 August 2021; published 11 October 2021)

A system of magnetic molecules coupled to microwave cavities (*LC* resonators) undergoes the equilibrium superradiant phase transition. The transition is experimentally observable. The effect of the coupling is first illustrated by the vacuum-induced ferromagnetic order in a quantum Ising model and then by the modification of the magnetic phase diagram of Fe_8 dipolar crystals, exemplifying the cooperation between intrinsic and photon-induced spin-spin interactions. Finally, a transmission experiment is shown to resolve the transition, measuring the quantum electrodynamical control of magnetism.

DOI: 10.1103/PhysRevLett.127.167201

In 1973, Hepp and Lieb showed that $N \to \infty$ polar molecules located inside a resonant electromagnetic cavity undergo a second order transition from a normal to a superradiant phase. The $\mathbb{Z}_2$ (parity) symmetry is spontaneously broken leading to a ferroelectriclike state in the "matter" and to a nonzero population of photons in the cavity at equilibrium [1–3]. However, 47 years and a global pandemic later, this quantum phase transition is yet to be measured [4]. During this time, the community has enjoyed a winding succession of proposals on how to achieve the superradiant phase transition (SPT), each shortly matched by its corresponding no-go theorem [5–10]. Nowadays, the nonobservation of the phase transition is well understood. The crux of the matter resides in the approximations used to derive the Hamiltonian solved by Hepp and Lieb, the so-called Dicke model. On one side, there is the treatment of the A^2 term (the diamagnetic term) [11]. On the other, matter truncations in different gauges must be done consistently as pointed out by Keeling, showing that the phase transition, if any, is completely attributable to matter interactions [12]. Consequently, the matter phase diagram remains unaltered despite it being immersed in a cavity and no photonic population develops. The same conclusion has been recently revisited [13]. A final step for closing the debate is found in the work by Andolina and collaborators [14]. In the thermodynamic limit $N \to \infty$, their no-go theorem illustrates how Gauge invariance inherently prohibits the SPT for electric dipoles in the long-wavelength limit. The latter implies that matter cannot respond to a static and uniform electromagnetic field. Therefore, to make the SPT observable, either the nature of the coupling or the spatial field distribution must be, in some way, modified.

Theoretical proposals consider systems in the ultrastrong light-matter coupling regime [15] or use electron gases that either possess a Rashba spin-orbit coupling [16] or are subjected to a spatially varying electromagnetic field [16–18] or have the role of photons be played by magnons [19].

Here, we propose an alternative setup, based on magnetic molecules that couple to superconducting microwave resonators via the Zeeman interaction [20]. Artificial magnetic molecules [21,22], designed and synthesized by chemical methods, consist of a high-spin cluster core surrounded and stabilized by a cloud of organic molecular ligands. The ability to chemically tune their relevant properties, such as the ground state spin, magnetic anisotropy and mutual interactions, combined with their stability as isolated molecular units, confer them a potential interest as magnetic memories in spintronic devices [23] and as qubits for scalable quantum information schemes [24–26]. Besides, they tend to organize forming crystals, which makes them model systems to study pure magnetic dipolar order and quantum phase transitions [27–31].

This work explores the realization of the Dicke model (and generalizations of it), which undergoes the equilibrium SPT, in a crystal of molecular nanomagnets coupled to a on-chip microwave cavity. We compute the critical condition that triggers the SPT at zero and finite temperatures under rather general conditions, e.g., for a spatially varying magnetic field or in the presence of direct molecule-molecule interactions, and discuss a feasible method to detect it. Besides, we build the phase diagram for the purely cavity-driven ferromagnetism and study how the spin-photon coupling enhances the intrinsic ferromagnetic order of a crystal of Fe_8 molecular clusters [31].

Magnetic cavity QED.—Hybrid platforms coupling electron [32] and, particularly, spin [33,34] ensembles to superconducting resonators or cavities complement circuit QED. Here, the "spins" are superconducting qubits [35,36]. Different magnetic species have been studied in this context, including impurity spins in semiconductors [37–39], lanthanide ions [40,41] and magnetic molecules [42–45]. To observe the SPT, set ups hosting molecular

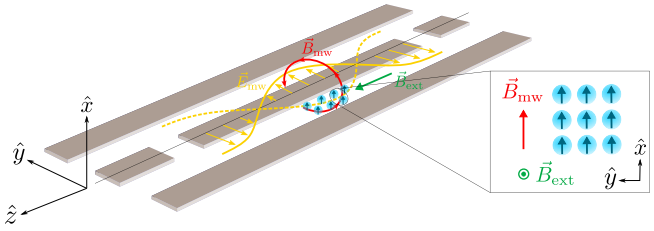

FIG. 1. Schematic picture of a coplanar waveguide (CPW) resonator coupled to a spin ensemble. $\boldsymbol{E}_{\rm mw}$ and $\boldsymbol{B}_{\rm mw}$ are the cavity's microwave electric and magnetic fields, respectively. $\boldsymbol{B}_{\rm ext}$ is the external magnetic field that induces a Zeeman splitting between the spin energy levels.

crystals offer the crucial advantage of coupling a macroscopic number of identical and perfectly organized spins to a single cavity mode (cf. Fig. 1).

A vast majority of molecular nanomagnets are both neutral and exhibit a close to zero electric dipole. Their response to external stimuli is then accurately described by a simple "giant"-spin effective Hamiltonian $\mathcal{H}_S$, which includes the effects of magnetic anisotropy and the couplings to magnetic field $\boldsymbol{B}$ [20,21]. The latter enter $\mathcal{H}_S$ via the Zeeman term $\mathcal{H}_Z = -g_e\mu_B \boldsymbol{S}\cdot\boldsymbol{B}$. Here $[S_i, S_j] = i\epsilon_{ijk}S_k$ are spin operators, $\mu_B = (e\hbar/2m)$ is the Bohr magneton, and g_e the Landé factor ($= 2$ for an electron spin). The diamagnetic response, which arises mainly from the molecular ligands surrounding the magnetic core, is much smaller that the paramagnetic one and can be safely neglected, especially at sufficiently low temperatures. These results provide the experimental background for the following discussion.

Let us summarize the main steps to model the molecules-cavity system in the single mode case. For the multimode case, see [46]. The electromagnetic field is quantized, yielding the cavity Hamiltonian $\mathcal{H}_c = \hbar\Omega a^\dagger a$, with a ($a^\dagger$) the photonic annihilation (creation) operators, $[a, a^\dagger] = 1$. The resonance frequency Ω ranges typically between 1 and 10 GHz. The local quantized magnetic field generated by the superconducting currents can be written as $\boldsymbol{B}_{\rm mw}(\boldsymbol{r}) = \boldsymbol{B}_{\rm rms}(\boldsymbol{r})(a^\dagger + a)$, with $B^2_{\rm rms}(\boldsymbol{r}) = \langle 0|B^2_{\rm mw}(\boldsymbol{r})|0\rangle$ its zero-point fluctuations.

The resulting gauge-invariant cavity-spin Hamiltonian can be written as follows [20,51]

$$\begin{aligned}\mathcal{H} &= \mathcal{H}_S + \mathcal{H}_c + \mathcal{H}_I,\\ &= \mathcal{H}_S + \hbar\Omega a^\dagger a + \sum_j \frac{\hbar\lambda_j}{\sqrt{N}}(e^{i\theta_j}S_j^+ + \text{H.c.})(a^\dagger + a),\end{aligned} \tag{1}$$

with N being the number of spins, the ladder operators $S^\pm = S^x \pm iS^y$, and the coupling constants

$$\frac{\lambda_j}{\sqrt{N}} = \frac{g_e\mu_B}{2\hbar}|B_{\rm rms}(\boldsymbol{r}_j)|. \tag{2}$$

Here, $\boldsymbol{r}_j$ is the position vector of the jth spin. The phases θ_j in Eq. (1) are defined through $B_{{\rm rms},x}(\boldsymbol{r}_j) + iB_{{\rm rms},y}(\boldsymbol{r}_j) = |B_{\rm rms}(\boldsymbol{r}_j)|e^{i\theta_j}$. If the molecules are $S = 1/2$ noninteracting spins, like in a sufficiently diluted free radical sample, $\mathcal{H}_S = \hbar(\omega_z/2)\sum_j \sigma_j^z$ and the Hamiltonian (1) matches exactly the Dicke model. Notice that this model does not suffer from the "A^2 issue" because the coupling is of Zeeman kind, rather than minimal (electric). Besides, the truncation of the electronic degrees of freedom to a finite dimensional Hilbert space is not an approximation but follows from the fact that we are dealing with "real" spins obeying the angular momentum commutation relations. Both properties combined permit to avoid the no-go theorems for the SPT [14].

Exact results at $N \to \infty$.—In order to study specific spin models and how their properties are affected by the coupling to light and vice versa, it is convenient to obtain an effective spin Hamiltonian where the light degrees of freedom have been traced out. Following Hepp and Lieb's original derivation [2], this effective Hamiltonian is defined by the following expression, exact in the $N \to \infty$ limit,

$$\bar{Z} = Tr_S\left(\frac{1}{\pi}\int d^2\alpha e^{-\beta\mathcal{H}(\alpha)}\right) = Tr_S(e^{-\beta\mathcal{H}_{S,\rm eff}}), \tag{3}$$

where $\mathcal{H}(\alpha) = \langle\alpha|\mathcal{H}|\alpha\rangle$ and $\mathcal{H}$ is the total Hamiltonian given by Eq. (1). The resulting (see [46]) effective Hamiltonian is

$$\mathcal{H}_{S,\rm eff} = \mathcal{H}_S - \frac{1}{\hbar\Omega}\left[\sum_j \frac{\hbar\lambda_j}{\sqrt{N}}(e^{i\theta_j}S_j^+ + \text{H.c.})\right]^2. \tag{4}$$

It is apparent that the light-matter coupling translates into an effective Ising-type ferromagnetic interaction among all spins that drives the quantum phase transition. This formulation is particularly handy for studying spin models that are well captured by a mean field approach, as we show below.

The critical point can be obtained by noticing that $[\mathcal{H}_I, \mathcal{H}_c] \sim [\mathcal{H}_I, \mathcal{H}_S] \sim 1/N$. Then, in the thermodynamic limit, system and cavity factorize. Generalizing the prescription in [14] to the finite temperature case (fully developed in [46]), the critical condition can be written in terms of the static response function $\mathcal{R}(T)$ of the bare spin model,

$$|\mathcal{R}(T)| \geq \frac{\hbar\Omega}{2}, \tag{5}$$

where

$$\mathcal{R}(T) = -\frac{\sum_{m,n} e^{-\beta\epsilon_m}|\langle\psi_m|\sum_j \frac{\hbar\lambda_j}{\sqrt{N}}(e^{i\theta_j}S_j^+ + \text{H.c.})|\psi_n\rangle|^2 \frac{e^{\beta\Delta_{mn}}-1}{\Delta_{mn}}}{\sum_m e^{-\beta\epsilon_m}}, \tag{6}$$

with $|\psi_m\rangle$, ϵ_m the eigenstates and eigenenergies of the bare spin Hamiltonian $\mathcal{H}_S$ and $\Delta_{mn} = \epsilon_m - \epsilon_n$. In the case of uniform coupling, $\lambda_i \equiv \lambda$, the static response function is proportional to the magnetic susceptibility $\mathcal{R} = (\lambda\hbar)^2\chi_\perp$ in the xy plane, perpendicular to the external dc magnetic field (see Fig. 1). A similar condition is found in three-dimensional electronic systems when the spin degrees of freedom are considered [18].

Both approaches show a relation between light and matter observables given by

$$\langle a\rangle = \frac{1}{\hbar\Omega}\left\langle \sum_j \frac{\hbar\lambda_j}{\sqrt{N}}(e^{i\theta_j}S_j^+ + \text{H.c.})\right\rangle_S, \tag{7}$$

indicating that the phase transition is marked by the onset of both a macroscopic population of photons in the cavity and a spontaneous magnetization in the spin system.

In the case of independent spins coupled to a field pointing along x, we obtain the critical condition of the Dicke model for a spin S

$$\bar{\lambda}^2 = \frac{\omega_z\Omega}{4}\left[(2S+1)\text{cth}\left(\hbar\beta\frac{\omega_z}{2}(2S+1)\right) - \text{cth}\left(\hbar\beta\frac{\omega_z}{2}\right)\right]^{-1}, \tag{8}$$

which depends on the coupling only through the collective parameter $\bar{\lambda}^2 \equiv N^{-1}\sum_j \lambda_j^2$, i.e., the root mean square of the spin-dependent couplings

$$\bar{\lambda}^2 = V_{\text{sample}}^{-1}\int_{V_{\text{sample}}} \lambda^2(\boldsymbol{r})dV = \frac{g_e^2\mu_B^2\mu_0}{8\hbar}\rho\nu\Omega, \tag{9}$$

where V_{sample} is the cavity volume occupied by spins and $\rho = N/V_{\text{sample}}$ is the density of spins. In the second equality, we have used Eq. (2) and the Virial theorem and introduced the filling factor $\nu = I(V_{\text{sample}})/I(V_{\text{total}})$ with $I(V) = \int_V |B_{\text{rms}}(\boldsymbol{r})|^2 dV$.

Vacuum-fluctuations-driven ferromagnetism.—To illustrate the effects of the coupling between the cavity and the magnetic molecules as well as the interplay between intrinsic and light-induced ferromagnetic interactions, we showcase two examples using realistic experimental parameters. From a theoretical perspective, Fig. 2 shows the alterations to the zero-temperature phases of the paradigmatic quantum Ising chain for $S = 1/2$ spins, defined by $\mathcal{H}_S = \mathcal{H}_{\text{Ising}} = (\hbar\omega_z/2)\sum_j \sigma_j^z - (J/2)\sum_i \sigma_i^x\sigma_{i+1}^x$. Note that according to Eq. (7) ferromagnetic and superradiant phases are synonymous; i.e., ferromagnetic ordering is always accompanied by a finite photon population in the cavity. In particular, regions I, II, and III are superradiant, as evidenced by the finite values of magnetization $|\langle\sigma_x\rangle|$ and photon number $\langle a^\dagger a\rangle/N$ shown in the insets of Fig. 2. Remarkably, the light-induced effective ferromagnetic interaction overpowers the intrinsic antiferromagnetic interaction

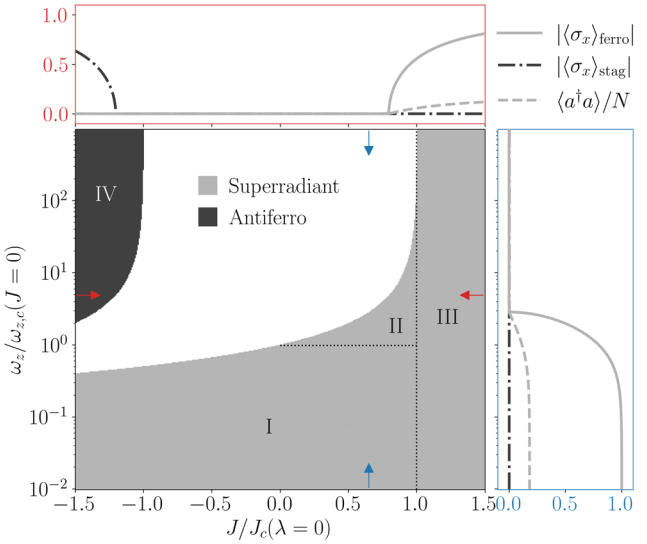

FIG. 2. Mean field phase diagram of the cavity-spin Hamiltonian for $S = 1/2$ spins with $\mathcal{H}_S = \mathcal{H}_{\text{Ising}}$ in 1D. The black region is antiferromagnetic. The grey region is superradiant and thus ferromagnetic. The white region is not superradiant nor magnetically ordered. For clarity, right and upper subplots showcase the standard $\langle\sigma_x\rangle$ and staggered $\langle\sigma_x\rangle_{\text{stag}}$ magnetizations, as well as the number of photons per spin $\langle a^\dagger a\rangle/N$, along vertical and horizontal slices of the phase diagram indicated by the arrows. For the units, $J_c(\lambda = 0)$ is the critical Ising coupling in the absence of cavity and $\omega_{z,c}(J = 0)$ is the critical spin frequency in the absence of direct Ising coupling. The parameters used are $\rho = 5.1 \times 10^{20}$ cm^{-3}, $\Omega = 1.4 \times 10^9$ s^{-1}, and $\nu = 1$.

extending region I into the $J < 0$ sector. In region II it is the synergy between intrinsic and induced ferromagnetism that gives rise to superradiance. Finally, region III is intrinsically ferromagnetic even in the absence of the cavity and thus becomes superradiant when coupled to one. The use of the mean field approximation is validated in [46] by comparing the superradiant phase boundary obtained with mean field against the one obtained using exact diagonalization to compute the response function $\mathcal{R}$ (5).

Next, we consider a more realistic model. It corresponds to a specific molecular material, a crystal of Fe_8 clusters with $S = 10$, which shows a ferromagnetic phase transition purely induced by dipolar interactions below a critical temperature $T_c(B_\perp = 0) \cong 0.6$ K and a zero-temperature critical magnetic field $B_{\perp,c} \simeq 2.65$ T [31]. The magnetic phase diagram measured for a magnetic field perpendicular to the magnetic anisotropy axis is shown in Fig. 3. As expected for a system dominated by long-range dipolar interactions, it agrees very well with the predictions of a mean-field Hamiltonian

$$\mathcal{H}_S = -DS_x^2 + E(S_z^2 - S_y^2) - g_e\mu_B\vec{B}\cdot\vec{S} - 2J\langle S_x\rangle S_x + J\langle S_x\rangle^2, \tag{10}$$

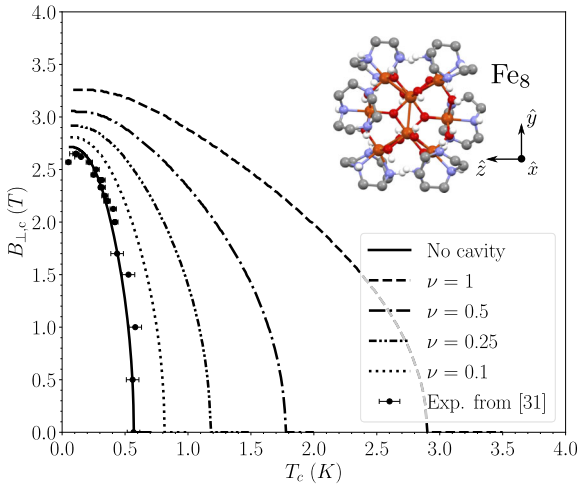

FIG. 3. $B_c - T_c$ phase boundary determined with a quantum mean-field calculation. The solid line corresponds to the bare spin model (10) and is verified against experimental data (dots) obtained for a crystal of Fe_8 molecular clusters [31], whose structure [52] is shown in the inset. The external field, $\boldsymbol{B}$, is applied perpendicular to the easy magnetization axis x: $\boldsymbol{B} = B_\perp(0, \sin\phi, -\cos\phi)$ with $\phi = 68°$. The magnetic anisotropy parameters are $D/k_B = 0.294$ K and $E/k_B = 0.046$ K, and the coupling $J/k_B = 2.85 \times 10^{-3}$ K. The remaining lines are obtained with the same method taking into account the coupling to a microwave cavity for a range of filling factors ν. The parameters used are $\rho = 5.1 \times 10^{20}$ cm^{-3}, taken from the crystal lattice of Fe_8 and $\Omega = 1.4 \times 10^9$ s^{-1}.

with parameters given in Fig. 3. The combination of high spin, thus high susceptibility, and negligible exchange interactions, which lead to a quite low T_c even for a densely concentrated spin lattice, makes this material well suited to obtain and measure the SPT.

This expectation is borne out by calculations that include the coupling to a microwave cavity, whose results are also included in Fig. 3. They show that light-matter interaction has a remarkable effect on the equilibrium phase diagram, enhancing both $B_{\perp,c}$ and T_c, the latter by almost as much as a factor of 6, depending on the filling of the cavity. This can be understood by noting that the effective Hamiltonian is given by Eq. (10) but with the coupling J replaced by $J_{\text{eff}} = J + \hbar\bar{\lambda}^2/\Omega$. This enhancement evidences that the cavity induces quite strong ferromagnetic correlations, a characteristic signature of the SPT, which in this case cooperate with the intrinsic interactions between the spins in the crystal. Achieving filling factors well above 0.1 seems quite reasonable provided that one achieves a sufficiently good interface between the chip and the magnetic material. It can also be seen from these results that, even after the introduction of direct spin-spin interactions, the transition depends only on the filling factor, as shown in [46]. We emphasize that the two previous examples show how, with magnetic coupling, the light-induced and intrinsic interactions add up, modifying the bare matter phase diagram. This is the signature of photon condensation and, thus, of the occurrence of the SPT [12,14].

Transmission experiment for resolving the transition.— Finally, we discuss how to measure a signature of the phase transition. A direct route would be to measure the order temperature of the magnetic material inside and outside the cavity. However, conventional methods to measure T_c (or B_c), based on magnetic susceptibility or neutron diffraction [31], do not lend themselves easily to include a superconducting cavity. Besides, they require very large crystals, often much larger than the typical cavity volumes. Therefore, we envision here a more accessible way: a transmission experiment, where the cavity is coupled to a microwave transmission line. A signal, sent through it, interacts with the cavity-spins system and the transmitted signal is recorded. Since this signal is proportional to the dynamical response of the system, we expect to observe a signature near the transition. Technically, the calculation involves computing the dynamical susceptibility of the whole system (cavity plus spins) using a quantum master equation. Typically, the dissipation for both the spins and the cavity is added phenomenologically, inserting the terms as if the cavity and the spins were not coupled. However, this so-called local approach has been criticized. A rigorous derivation involves taking into account the coupling between the two subsystems, obtaining the global master equation. The differences between both approaches are relevant in strongly coupled systems [53–55]. Since we are interested in what happens near the transition, we explore the differences between local and global approaches to rule out that the signature is an artifact of the approximations taken. We notice, however, that in the global approach both eigenvectors and eigenvalues for the coupled system are needed. These are impossible to obtain in a full treatment. On the other hand, if we consider a spin $1/2$ Dicke model with homogeneous coupling to the cavity a Holstein-Primakoff transformation allows us to write the total Hamiltonian as two coupled oscillators. Then, the system is exactly solvable and the global master equation can be obtained. By doing so, we can compare both local and global approaches for resolving the transition.

The explicit formulas are rather involved and thus sent to [46]. In Fig. 4 we summarize our findings. We show 2D transmission plots for temperatures larger or smaller than the zero-field critical temperature $T_c(0)$. In the former limit, the system remains disordered, regardless of ω_z and only shows the well-known avoided crossing at $\omega = \Omega = \omega_z$. As temperature is decreased below $T_c(0)$ the magnetic and photon states depend on ω_z. The phase transition, for $\omega_z \sim \omega_{z,c}(0)$, is then characterized by the appearance of a new resonance, i.e., a new transmission channel, at $\omega_z \sim \omega_{z,c}(0)$. On physical grounds, this is a consequence of the vanishing frequency of the lower mode at the transition, which increases the response at

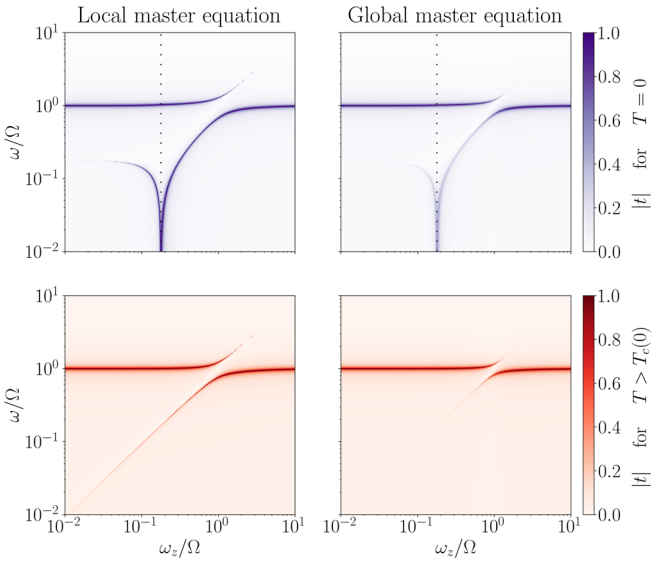

FIG. 4. Plots of the transmission for temperatures below and above the critical temperature at zero field (top and bottom) computed with the local and global master equation (left and right) as a function of the ratios between ω, ω_z, and Ω for a spin $1/2$ Dicke model. A dotted black line marks the transition to the superradiant phase at $\omega_{z,c}(0)$. The parameters used are $\gamma_1 = 0.025\ \Omega$, $\gamma_2 = 0.025\omega_z$, $\rho = 5.1\times10^{20}\,\mathrm{cm}^{-3}$, $\Omega = 1.4\times10^{9}\ \mathrm{s}^{-1}$, and $\nu = 0.25$.

equilibrium ($\omega \to 0$). Besides, the resonance appears in both the local and global approaches, supporting our findings. Quantitative differences appear, obviously, but this is expected since one of the pitfalls of the local approach is not reproducing the correct equilibrium states. This behavior constitutes a clear signature of the SPT and shows that this transition can be detected in a standard temperature-dependent transmission experiment, provided that the spin-photon coupling is large enough.

Conclusions.—We have shown that the coupling of a macroscopic number of spins, in particular crystals of molecular nanomagnets, to the quantum vacuum fluctuations of cavities or *LC* resonators generates ferromagnetic spin-spin interactions that lead to an equilibrium superradiant phase transition. Using realistic parameters, we find that it also gives rise to detectable signatures in the transmission of microwaves through such a hybrid setup, thus providing a feasible solution to the long-standing problem of measuring the SPT. Our results also present these systems as ideal for exploring the quantum electrodynamical control of matter, baptized as cavity QED materials [56]. Recent studies have shown that quantum light fluctuations can modify properties such as excitonic transport [57–59], chemical reactivity [60,61], superconductivity [62–65], and the ferroelectric phase in quantum paramagnetic materials [66–68]. Here, we show that they can also generate, modify and control long-range ordered magnetic phases.

The authors acknowledge funding from the EU (COST Action 15128 MOLSPIN, QUANTERA SUMO and FET-OPEN Grant No. 862893 FATMOLS), the Spanish MICINN (Grants No. MAT2017-88358-C3-1-R, No. RTI2018-096075-B-C21, No. PCI2018-093116, and No. EUR2019-103823), the Gobierno de Aragón (Grant No. E09-17R Q-MAD), and the BBVA foundation (Leonardo Grants 2018).

[1] K. Hepp and E. H. Lieb, Ann. Phys. (N.Y.) **76**, 360 (1973).
[2] K. Hepp and E. H. Lieb, Phys. Rev. A **8**, 2517 (1973).
[3] Y. K. Wang and F. T. Hioe, Phys. Rev. A **7**, 831 (1973).
[4] P. Kirton, M. M. Roses, J. Keeling, and E. G. D. Torre, Adv. Quantum Technol. **2**, 1800043 (2018).
[5] K. Rzażewski, K. Wódkiewicz, and W. Żakowicz, Phys. Rev. Lett. **35**, 432 (1975).
[6] P. Nataf and C. Ciuti, Nat. Commun. **1**, 72 (2010).
[7] O. Viehmann, J. von Delft, and F. Marquardt, Phys. Rev. Lett. **107**, 113602 (2011).
[8] D. Hagenmüller and C. Ciuti, Phys. Rev. Lett. **109**, 267403 (2012).
[9] L. Chirolli, M. Polini, V. Giovannetti, and A. H. MacDonald, Phys. Rev. Lett. **109**, 267404 (2012).
[10] A. Vukics, T. Grießer, and P. Domokos, Phys. Rev. Lett. **112**, 073601 (2014).
[11] L. Garziano, A. Settineri, O. Di Stefano, S. Savasta, and F. Nori, Phys. Rev. A **102**, 023718 (2020).
[12] J. Keeling, J. Phys. Condens. Matter **19**, 295213 (2007).
[13] A. Stokes and A. Nazir, Phys. Rev. Lett. **125**, 143603 (2020).
[14] G. M. Andolina, F. M. D. Pellegrino, V. Giovannetti, A. H. MacDonald, and M. Polini, Phys. Rev. B **100**, 121109(R) (2019).
[15] D. De Bernardis, T. Jaako, and P. Rabl, Phys. Rev. A **97**, 043820 (2018).
[16] P. Nataf, T. Champel, G. Blatter, and D. M. Basko, Phys. Rev. Lett. **123**, 207402 (2019).
[17] D. Guerci, P. Simon, and C. Mora, Phys. Rev. Lett. **125**, 257604 (2020).
[18] G. M. Andolina, F. M. D. Pellegrino, V. Giovannetti, A. H. MacDonald, and M. Polini, Phys. Rev. B **102**, 125137 (2020).
[19] M. Bamba, X. Li, N. M. Peraca, and J. Kono, arXiv: 2007.13263.
[20] M. Jenkins, T. Hümmer, M. J. Martínez-Pérez, J. García-Ripoll, D. Zueco, and F. Luis, New J. Phys. **15**, 095007 (2013).
[21] D. Gatteschi, R. Sessoli, and J. Villain, *Molecular Nanomagnets* (Oxford University Press, New York, 2006), Vol. 5.
[22] J. Bartolomé, F. Luis, and J. F. Fernández, *Molecular Magnets: Physics and Applications* (Springer, Berlin, Heildelberg, 2016).
[23] L. Bogani and W. Wernsdorfer, Nat. Mater. **7**, 179 (2008).
[24] E. Moreno-Pineda, C. Godfrin, F. Balestro, W. Wernsdorfer, and M. Ruben, Chem. Soc. Rev. **47**, 501 (2018).
[25] A. Gaita-Ariño, F. Luis, S. Hill, and E. Coronado, Nat. Chem. **11**, 301 (2019).

[26] M. Atzori and R. Sessoli, J. Am. Chem. Soc. **141**, 11339 (2019).
[27] J. F. Fernández and J. J. Alonso, Phys. Rev. B **62**, 53 (2000).
[28] A. Morello, F. L. Mettes, F. Luis, J. F. Fernández, J. Krzystek, G. Aromí, G. Christou, and L. J. de Jongh, Phys. Rev. Lett. **90**, 017206 (2003).
[29] F. Luis, J. Campo, J. Gómez, G. J. McIntyre, J. Luzón, and D. Ruiz-Molina, Phys. Rev. Lett. **95**, 227202 (2005).
[30] B. Wen, P. Subedi, L. Bo, Y. Yeshurun, M. P. Sarachik, A. D. Kent, A. J. Millis, C. Lampropoulos, and G. Christou, Phys. Rev. B **82**, 014406 (2010).
[31] E. Burzurí, F. Luis, B. Barbara, R. Ballou, E. Ressouche, O. Montero, J. Campo, and S. Maegawa, Phys. Rev. Lett. **107**, 097203 (2011).
[32] M. Ruggenthaler, N. Tancogne-Dejean, J. Flick, H. Appel, and A. Rubio, Nat. Rev. Chem. **2**, 0118 (2018).
[33] Z.-L. Xiang, S. Ashhab, J. Q. You, and F. Nori, Rev. Mod. Phys. **85**, 623 (2013).
[34] A. A. Clerk, K. W. Lehnert, P. Bertet, J. R. Petta, and Y. Nakamura, Nat. Phys. **16**, 257 (2020).
[35] A. Wallraff, D. I. Schuster, A. Blais, L. Frunzio, R.-S. Huang, J. Majer, S. Kumar, S. M. Girvin, and R. J. Schoelkopf, Nature (London) **431**, 162 (2004).
[36] A. Blais, A. L. Grimsmo, S. M. Girvin, and A. Wallraff, Rev. Mod. Phys. **93**, 025005 (2021).
[37] Y. Kubo, F. R. Ong, P. Bertet, D. Vion, V. Jacques, D. Zheng, A. Dréau, J.-F. Roch, A. Auffeves, F. Jelezko, J. Wrachtrup, M. F. Barthe, P. Bergonzo, and D. Esteve, Phys. Rev. Lett. **105**, 140502 (2010).
[38] D. I. Schuster, A. P. Sears, E. Ginossar, L. DiCarlo, L. Frunzio, J. J. L. Morton, H. Wu, G. A. D. Briggs, B. B. Buckley, D. D. Awschalom, and R. J. Schoelkopf, Phys. Rev. Lett. **105**, 140501 (2010).
[39] S. Weichselbaumer, P. Natzkin, C. W. Zollitsch, M. Weiler, R. Gross, and H. Huebl, Phys. Rev. Applied **12**, 024021 (2019).
[40] P. Bushev, A. K. Feofanov, H. Rotzinger, I. Protopopov, J. H. Cole, C. M. Wilson, G. Fischer, A. Lukashenko, and A. V. Ustinov, Phys. Rev. B **84**, 060501(R) (2011).
[41] S. Probst, A. Tkalčec, H. Rotzinger, D. Rieger, J.-M. L. Floch, M. Goryachev, M. E. Tobar, A. V. Ustinov, and P. A. Bushev, Phys. Rev. B **90**, 100404(R) (2014).
[42] C. Bonizzoni, A. Ghirri, M. Atzori, L. Sorace, R. Sessoli, and M. Affronte, Sci. Rep. **7**, 13096 (2017).
[43] M. Mergenthaler, J. Liu, J. J. Le Roy, N. Ares, A. L. Thompson, L. Bogani, F. Luis, S. J. Blundell, T. Lancaster, A. Ardavan, G. A. D. Briggs, P. J. Leek, and E. A. Laird, Phys. Rev. Lett. **119**, 147701 (2017).
[44] I. Gimeno, W. Kersten, M. C. Pallarés, P. Hermosilla, M. J. Martínez-Pérez, M. D. Jenkins, A. Angerer, C. Sánchez-Azqueta, D. Zueco, J. Majer, A. Lostao, and F. Luis, ACS Nano **14**, 8707 (2020).
[45] C. Bonizzoni, A. Ghirri, F. Santanni, M. Atzori, L. Sorace, R. Sessoli, and M. Affronte, npj Quantum Inf. **6**, 68 (2020).
[46] See the Supplemental Material at http://link.aps.org/supplemental/10.1103/PhysRevLett.127.167201 for additional information on the modeling of the interaction between light and molecules, the effective spin Hamiltonian, the critical condition in terms of the spin static response function, the finite temperature stiffness theorem, the calculation of the modified Ising phase diagram, the dependence of the effective spin-spin interaction on $\bar{\lambda}$ and the transmission experiment, which includes Refs. [47–50].
[47] E. H. Lieb, Commun. Math. Phys. **31**, 327 (1973).
[48] G. Giuliani and G. Vignale, *Quantum Theory of the Electron Liquid* (Cambridge University Press, Cambridge, England, 2005).
[49] H. P. Breuer and F. Petruccione, *The Theory of Open Quantum Systems* (Oxford University Press, Oxford, 2002).
[50] C. Emary and T. Brandes, Phys. Rev. E **67**, 066203 (2003).
[51] M. D. Jenkins, D. Zueco, O. Roubeau, G. Aromí, J. Majer, and F. Luis, Dalton Trans. **45**, 16682 (2016).
[52] K. Weighardt, K. Pohl, I. Jibril, and G. Huttner, Angew. Chem., Int. Ed. Engl. **23**, 77 (1984).
[53] P. P. Hofer, M. Perarnau-Llobet, L. D. M. Miranda, G. Haack, R. Silva, J. B. Brask, and N. Brunner, New J. Phys. **19**, 123037 (2017).
[54] C. Ciuti and I. Carusotto, Phys. Rev. A **74**, 033811 (2006).
[55] J. O. González, L. A. Correa, G. Nocerino, J. P. Palao, D. Alonso, and G. Adesso, Open Syst. Inf. Dyn. **24**, 1740010 (2017).
[56] V. Rokaj, M. Ruggenthaler, F. G. Eich, and A. Rubio, arXiv:2006.09236.
[57] J. Feist and F. J. Garcia-Vidal, Phys. Rev. Lett. **114**, 196402 (2015).
[58] J. Schachenmayer, C. Genes, E. Tignone, and G. Pupillo, Phys. Rev. Lett. **114**, 196403 (2015).
[59] E. Orgiu, J. George, J. A. Hutchison, E. Devaux, J. F. Dayen, B. Doudin, F. Stellacci, C. Genet, J. Schachenmayer, C. Genes, G. Pupillo, P. Samorì, and T. W. Ebbesen, Nat. Mater. **14**, 1123 (2015).
[60] A. Thomas, J. George, A. Shalabney, M. Dryzhakov, S. J. Varma, J. Moran, T. Chervy, X. Zhong, E. Devaux, C. Genet, J. A. Hutchison, and T. W. Ebbesen, Angew. Chem., Int. Ed. Engl. **55**, 11462 (2016).
[61] A. Thomas, L. Lethuillier-Karl, K. Nagarajan, R. M. A. Vergauwe, J. George, T. Chervy, A. Shalabney, E. Devaux, C. Genet, J. Moran, and T. W. Ebbesen, Science **363**, 615 (2019).
[62] M. A. Sentef, M. Ruggenthaler, and A. Rubio, Sci. Adv. **4**, eaau6969 (2018).
[63] F. Schlawin, A. Cavalleri, and D. Jaksch, Phys. Rev. Lett. **122**, 133602 (2019).
[64] J. B. Curtis, Z. M. Raines, A. A. Allocca, M. Hafezi, and V. M. Galitski, Phys. Rev. Lett. **122**, 167002 (2019).
[65] A. Thomas, E. Devaux, K. Nagarajan, T. Chervy, M. Seidel, D. Hagenmüller, S. Schütz, J. Schachenmayer, C. Genet, G. Pupillo, and T. W. Ebbesen, arXiv:1911.01459.
[66] P. Pilar, D. D. Bernardis, and P. Rabl, Quantum **4**, 335 (2020).
[67] M. Schuler, D. D. Bernardis, A. M. Läuchli, and P. Rabl, SciPost Phys. **9**, 66 (2020).
[68] Y. Ashida, A. Imamoglu, J. Faist, D. Jaksch, A. Cavalleri, and E. Demler, Phys. Rev. X **10**, 041027 (2020).